

THERMAL FLUCTUATIONS AND THE STRUCTURE OF MICROEMULSIONS

S. A. Safran, D. Roux^(a), M. E. Cates^(b), and D. Andelman^(c)

Corporate Research Science Labs
Exxon Research and Engineering Co.
Annandale, NJ 08801

We analyze the role of thermal fluctuations in determining the phase equilibria and structural properties of microemulsions. In the dilute limit, where the microemulsions are globular, the effects of thermal fluctuations are reviewed. To treat the case where the amounts of oil and water are comparable, a lattice model is used; each cell of size ξ is filled with either pure water or oil. Surfactant molecules are presumed to form an incompressible fluid monolayer at the oil-water interface. The monolayer is characterized by a size-dependent bending constant $K(\xi)$, which is small for $\xi \geq \xi_K$, the de Gennes-Taupin persistence length. The model predicts a middle phase microemulsion of structural length scale $\xi \approx \xi_K$ which coexists with dilute phases of surfactant in oil and surfactant in water. (These phases have $\xi \approx a$, a being a molecular length.) On the same ternary phase diagram, we find also two regions of two-phase equilibrium involving upper- and lower-phase microemulsions that coexist with either almost pure water or oil. At high temperatures and/or low values of the bare bending constant, $K_0 = K(a)$, we find a first-order transition between the random microemulsion and a lamellar phase as the surfactant concentration is increased. For low temperatures and/or high values of the bare bending constant, the middle-phase microemulsion may be entirely precluded by separation to a lamellar phase.

published in:

"Surfactants in Solutions", Ed. by
K. Mittal and B. Lindman
(Plenum, NY, 1989) Volume 10

I. INTRODUCTION

A. Microemulsions

Microemulsions are thermodynamically stable, fluid, oil-water-surfactant mixtures¹. The surfactant volume fraction is typically low (~5%); most microemulsions contain also co-surfactant (alcohol) and/or salt. A characteristic feature of microemulsions, as opposed to simple liquid mixtures, is that the oil and water remain separated in coherent domains, typically tens or hundreds of Angstroms in size. Because of their amphiphilic character, the surfactant molecules prefer the interfacial environment to either that of water or oil. This results in an extensive oil-water interface.

The configuration of the oil and water domains varies with composition. For small fractions of oil in water or of water in oil, the structure is that of globules^{2,3,4} whose colloidal properties are well understood⁵. However, when the volume fractions of oil and water are comparable, one expects random⁶, bicontinuous⁷ structures to form^{8,9,10}. Of course, under appropriate conditions (particularly when the volume fraction of surfactant is higher than a few percent) various ordered structures, such as lamellae, may also arise¹¹.

A characteristic feature is the presence of two- and three-phase regions in the phase diagram. In the two-phase regions there is coexistence between an almost pure phase (surfactant in oil or surfactant in water) and a microemulsion (lower- or upper-phase, respectively)¹². In the three-phase region, a middle-phase microemulsion coexists simultaneously with almost pure water and almost pure oil.

In special cases, the phase diagram is oil-water symmetric. This balance point is achieved under variation of a parameter such as salt concentration¹⁰. Such a parameter may be tuned so as to alter the spontaneous curvature of the surfactant film; it is commonly believed^{5,13} that at the symmetric (balance) point there is no preferred curvature of the monolayer. In addition, at the balance point, the middle phase microemulsion shows very low interfacial tensions¹⁴ ($\sigma \sim 10^{-3} - 10^{-5}$ dyne/cm) with both of the phases (which are nearly all water or oil) with which it coexists; this results in a variety of technological applications, for example, in chemically enhanced oil recovery¹⁵. Crudely one can argue that $\sigma \sim T/\xi^2$ where ξ is a structural length scale of order of the domain size and T is

the temperature. Since $\xi \sim 100 \text{ \AA}$, σ is much smaller than the interfacial tension between two molecular fluids.

There have so far been two differing approaches to the construction of thermodynamic models for microemulsions. In this paper we follow the "phenomenological" approach, which was initiated by Talmon and Prager⁶, and further developed by de Gennes and coworkers^{16,17} and Widom¹⁸. In this approach one regards oil and water as continuum liquids; the interfacial surfactant layer is treated either as a flexible sheet, or in a microscopic manner similar to that of insoluble Langmuir monolayers¹⁹. The presence of salt and/or alcohol is not directly treated, but enters through the energy parameters of the interfacial sheet. The strategy is to fix the volume fractions of oil, water, and surfactant, and to then calculate the free energy of a hypothetical homogeneous phase of this composition. This generates a free energy surface as a function of composition, from which the phase diagram can be determined. In calculating the free energy, it is often convenient to describe the oil and water domains in terms of a coarse-grained lattice; in this procedure, the lattice spacing remains comparable to the domain size, which is usually much larger than a molecular length scale.

The second approach is based on the construction of "microscopic" lattice models, in which a cell of the lattice contains only a small number of molecules. This approach was initiated by Wheeler and Widom²⁰; and has recently been extended by Widom²¹ and others²². This microscopic approach, though of undoubted fundamental interest, may be more difficult to implement than the phenomenological one²³. In particular, a microscopic model of microemulsions must produce structural organization on a length scale (the domain size) much larger than that of the lattice. It may, therefore, be argued that the microscopic approach is better suited to the description of long-range ordered mesophases, which occur at higher surfactant concentrations, than the description of random, bicontinuous structures, such as middle-phase microemulsions²⁴.

B. Thermal Fluctuations and Globular Microemulsions

The effect of thermal fluctuations on the properties of spherical⁴ and cylindrical³ microemulsions was calculated in the context of a continuum model of a surfactant monolayer at the oil/water interface. This is appropriate for globules whose size is much greater than a typical

surfactant dimension. The oil and water regions are assumed to be surfactant free, while the surfactant monolayer, which typically has an area per chain of $\sim 20\text{\AA}^2$, is assumed to be in the incompressible liquid state^{25,19}. The total energy is the sum of the curvature or bending energy of the individual droplets. The bending energy of a single globule is written^{3,4,26} as

$$F_b = \frac{K}{2} \int dS (c_1 + c_2 - c_0)^2 + \frac{\bar{K}}{2} \int dS (c_1 - c_2)^2 \quad (1.1)$$

In Eq. (1.1), the integral is over the globule surface S . The spontaneous curvature, c_0 positive or negative, describes the tendency of the surfactant monolayer to bend towards either the water or the oil respectively. The first term favors structures whose average curvature (c_1+c_2) is equal to the spontaneous curvature; deviations from this minimum energy state incur an energy cost parameterized by the bending elastic constant K . When the saddle-splay elastic constant $\bar{K} > 0$, the second term favors structures with equal radii of curvature in the two orthogonal directions.

For a system with a fixed amount of surfactant, the total surface area of all the globules (whose number density must be determined as part of the calculation) is fixed by the incompressibility assumption. In addition, the total volume enclosed by the globules is fixed by the concentrations of the internal water or oil. It is the competition between the tendency to make globules with the spontaneous curvature c_0 and the necessity to satisfy the incompressibility constraints which leads to the variety of structures that are predicted.

The phase diagram has been presented in Ref.3, where regions of stability for spherical, cylindrical, and lamellar phases are predicted as functions of the concentrations, the spontaneous curvature c_0 , and the ratio of \bar{K}/K . In the derivation of this phase diagram, it was assumed that all the globules are identical. However, the entropy of the surfactant monolayer results in an ensemble of globules whose sizes and shapes depart from the simple monodisperse set of spheres, cylinders, or lamellae calculated through the minimization of the bending energy. The probability that an arbitrary deformation of the globules will occur in thermal equilibrium is proportional to the Boltzmann factor $\exp(-\Delta F_b)$, where ΔF_b is the change in the bending energy due to the deformation. The magnitude of thermal fluctuations in the globular systems can then be calculated.

For spherical globules, the main effect of the thermal fluctuations is

polydispersity in size and shape fluctuations which are dominated by $l=2$ spherical harmonic modes. However, the integrity of the description of the system as a set of approximately monodisperse spheres is maintained, since these fluctuations have a magnitude which is on the order of $\sim 20\%$ rms deviation.

While the effects of thermal fluctuations on the ensemble of spherical globules is relatively minor, this is not the case for cylindrical or lamellar microemulsions. For the quasi-one-dimensional cylindrical structure, the effects of thermal fluctuations are the largest. The cylinders are only rigid on a length scale $\xi_c \sim K/T$ (the persistence length). On longer length scales, the cylinder axis wanders randomly in space.

This random wandering of the cylinder axis suggests a polymer-like description of the long-wavelength properties of the long, flexible microemulsions. The "molecular weight" of the polymers is self-consistently determined by the system and is not fixed by the kinetics of preparation as for simple, molecular polymers. Light scattering experiments have recently been interpreted with a polymer-like model for these systems²⁷. In addition, electron micrographs have yielded observations of flexible, cylindrical structures²⁸.

Lamellar structures are also affected by thermal fluctuations, as analyzed by de Gennes and Taupin¹⁶. By summing over undulation modes in a nearly flat sheet of bending constant K and zero surface tension, they calculated a persistence length defined by

$$\xi_K = a e^{4\pi K/\alpha T} \quad (1.2)$$

Here α is a numerical constant, which depends on the details of the calculations. (De Gennes and Taupin set $\alpha = 2$, but below we will find it convenient to use a different value.) In Eq.(1.2), a is a molecular size, which provides a lower cutoff in the wavelength of the undulations, and T is the temperature (we set Boltzmann's constant, k_B equal to unity). The sheet remains flat over distances $\xi < \xi_K$ but is crumpled at larger length scales. Note that the persistence length for lamellae is much larger than the corresponding ξ_c for cylinders for the same value of K/T , due to the weaker effect of thermal fluctuations in two-dimensions (lamellae) compared with one (cylinders). In Ref. 16 it is suggested that the persistence length is

related to the scale size in bicontinuous microemulsions and that the entropy of the random structure stabilizes the microemulsions against the ordered, lamellar phases. These ideas are supported by our calculations presented in this paper (and elsewhere²⁹) which establish a quantitative link between the phase behavior and the persistence length of random microemulsions.

C. Previous Phenomenological Models

As mentioned above, the first phenomenological model of disordered microemulsion was that of Talmon and Prager⁶. They considered a subdivision of space into random (Voronoi) polyhedra, which were filled at random with either oil or water, according to a probability proportional to the volume fraction of each component. The surfactant was presumed to form a monolayer at the interface between adjacent cells of water and oil; the area per surfactant molecule was taken as a fixed constant, $\Sigma = \Sigma_0$. The bending energy of the surfactant film was included (to some extent) by assuming the interface to be completely flat everywhere except at the edges of the Voronoi polyhedra. Three-phase coexistence was predicted, but only by assuming that the surfactant packing density is changed in the vicinity of the edges. The energetics of this change are not considered; neither is the harmonic bending energy used to describe the structures of membranes and liquid crystals. A further discussion of the Talmon-Prager formulation may be found in Ref. 17; despite various drawbacks, the model has proved very valuable as a starting point for improved phenomenological theories.

The first such improved theory was proposed by de Gennes and Taupin¹⁶, and studied in more detail by Jouffroy, Levinson and de Gennes (JLG)¹⁷. The JLG model drew on a physical picture of undulating lamellae described above. This model simplified the Talmon-Prager construction by dividing space into a lattice of cubes (rather than Voronoi polyhedra); the cubes are filled at random with oil or water according to their volume fractions. Based on the physical picture of the persistence length, they chose the lattice size to be always equal to ξ_K . Within the random mixing approximation, this requires that the interfacial area per surfactant molecule, Σ , depends on composition as

$$\Sigma \propto \frac{\phi(1-\phi)}{\phi_s \xi_K} \quad (1.3)$$

where ϕ is the volume fraction of water, $1-\phi$ is the volume fraction of oil

and ϕ_s is the volume fraction of surfactant. It is assumed that $\phi_s \ll \phi$, $1 - \phi$. JLG used a free energy contribution per surfactant molecule

$$F = A (\Sigma - \Sigma_0)^2 / \Sigma_0^2 \quad (1.4)$$

This represents the preference of the surfactant layer for an optimum area per molecule, Σ_0 . The bending energy was estimated by assuming the local radius of curvature of the interfacial film to be everywhere comparable to the lattice size ξ_k . (This improves the original Talmon-Prager formulation in which curvature is concentrated at the edges of the Voronoi polyhedra.)

The JLG model, while appealingly simple, does not predict three-phase equilibrium. Instead, there is a two-phase region involving equilibrium between two microemulsions. This is understood as follows: As the surfactant concentration decreases, a uniform phase of the required composition would have $\Sigma \gg \Sigma_0$ [Eq. (1.3)], with a corresponding energy penalty from (1.4) which can be avoided by phase separation into two phases, each having $\Sigma \approx \Sigma_0$. The line $\Sigma = \Sigma_0$ on the phase diagram, known as the Schulman line^{16,17} is everywhere close to the two-phase boundary. For high surfactant concentrations, this model predicts $\Sigma \ll \Sigma_0$; a pure surfactant phase is not allowed since it is assumed that the surfactant resides only at the oil/water interface.

The next development was the theory of Widom¹⁸. He introduced a (cubic) lattice of variable size ξ , which he then treated as a variational parameter; the free energy was taken at its minimum over ξ for each composition. In his calculation of the bending energy contributions, Widom essentially followed the formulation of JLG.

Widom departed slightly from JLG in the manner in which the variable interfacial area per surfactant, Σ , was treated. Specifically, he treated the interfacial layer as an ideal gas of surfactant in two dimensions. In conjunction with a bare interfacial tension γ between oil and water, this gives a quadratic minimum in the free energy as a function of the area per head Σ . This is basically the same as Eq.(1.4); however, the coefficient A in that expression is always of order T . Thus Widom's model describes a highly compressible surfactant film at the oil-water interface. While this may be appropriate under some conditions, there are other cases in which the surfactant layer is more like an incompressible two-dimensional liquid. For

example, measurements on globular and bicontinuous microemulsions²⁵ show that the interfacial area per polar head remains approximately constant under a wide range of conditions, even in the presence of cosurfactant; moreover, measurements on similar surfactants in a Langmuir geometry show that the Σ found directly from studies of microemulsions indeed corresponds to a relatively incompressible fluid state^{8,19}.

Nonetheless, Widom's model successfully predicts three-phase equilibrium involving a middle-phase microemulsion. For sensible choices of microscopic energy parameters, the predicted structural length scale ξ for the balanced middle phase is of order 100 Å, in accordance with experiments⁸. This middle phase coexists with two phases which are mostly oil or water, that have $\xi \approx a$, where a is a molecular cutoff. However, for $K/T \gg 1$, the prediction for ξ depends strongly on the bare oil-water surface tension, γ , but only weakly on the bending constant K of the surfactant film. This is mathematically unrelated to the expression (1.2) for the de Gennes-Taupin persistence length, ξ_K ; more important, it seems to be at variance with a range of experiments^{1,11} that indicate (albeit indirectly) that the properties of the middle phase depend very sensitively on the bending constant K . For example, to make a middle phase at all one usually requires cosurfactants such as alcohol, which are expected to reduce K significantly, while having very little effect on the bare surface tension.

D. The Present Work

Our model and its results have previously been summarized²⁹. We follow JLG and Widom in approximating the oil-water domain structure by a coarse-grained lattice. Similarly a random mixing approximation is used to calculate both the entropy of mixing of the domains, and the extent of the oil-water interface; it is assumed that all the surfactant resides at this interface. We depart from JLG, and follow Widom, in assigning to the lattice a variable cell size ξ ; however, rather than being a variational parameter, ξ will be determined uniquely by the volume fractions of oil, water and surfactant. This is because it is assumed that the surfactant layer at the oil-water interface as an incompressible two-dimensional fluid: $\Sigma = \Sigma_0$ is a fixed constant. The volume fraction of surfactant is then proportional to the total area of the oil-water interface, which is a known function of the water and oil volume fractions, and ξ , once the random mixing approximation, is made (see below).

Our second major departure from the previous formulations lies in the

treatment of the bending energy. Helfrich³⁰, and Peliti and Leibler³¹, have shown that the bending constant K of a flexible sheet of size ξ is renormalized downwards by thermal fluctuations at short length scales. In first-order perturbation theory, these authors found a size-dependent effective bending constant, $K(\xi)$, which obeys

$$K(\xi) = K_0 [1 - \tau \log(\xi/a)] \quad (1.5)$$

where $K_0 = K(a)$ is the bare bending constant (denoted previously by K); a is a molecular length which provides the cutoff wavelength of undulation modes [cf. Eq.(1.2)]; and

$$\tau = \alpha T / 4\pi K_0 \quad (1.6)$$

Here α is a numerical constant, whose precise value ($\alpha = 1$, or $\alpha = 3$) remains in dispute^{30,31,32}. In the remainder of this article, we will choose $\alpha=1$. It is convenient to choose Eq.(1.5) as a definition of the arbitrary parameter α in Eq.(1.2) for the persistence length, ξ_K . In this case, Eq.(1.5) becomes

$$K(\xi) = -\tau K_0 \log(\xi/\xi_K). \quad (1.7)$$

The downward renormalization of K indicates that it becomes relatively easy to bend a sheet of size $\xi \geq \xi_K$, since such a sheet is anyway spontaneously crumpled. The perturbative result (1.5) fails for $\xi \geq \xi_K$ since mechanical stability requires $K \geq 0$. However, for $\xi \leq \xi_K$ the form (1.5) should give the correct qualitative behavior.

Our model for microemulsions incorporates the renormalization of the bending constant by identifying the length scale ξ in Eq.(1.5) with the lattice constant used in the coarse graining of the oil and water domains. This captures the fact that there is little to be gained, in terms of bending energy, by having domains much larger than ξ_K , the persistence length of the surfactant film. This is because such a domain has a wrinkled surface, and so may as well break up into smaller pieces (thus gaining entropy of mixing). Of course it was precisely this physical idea that motivated JLG to set $\xi = \xi_K$ in their model; however that turned out to be too restrictive an assumption to give three-phase equilibrium, since when the compositions approach those of pure water or oil (as for the phases with which the middle phase coexists) the domains may be much smaller than

ξ_K . In our model, we find a middle phase microemulsion for which the structural length scale ξ is indeed comparable to ξ_K as defined by Eq.(1.2); but this is a result of the theory, rather than an initial assumption.

The organization of this paper is as follows: In section II we present a phenomenological model which combines features of both the JLG model and that of Widom. Section III describes extensions of our model to account more carefully for the properties of the mostly oil or water phases that coexist with the middle-phase microemulsion. In that section we also discuss the stability of the microemulsion relative to lamellar phases. Section IV contains a further discussion of our results. In Section V we present our conclusions and future prospects.

II. THE BASIC MODEL

A. Free Energy of a Random Microemulsion

With the assumptions of the previous section, we consider microemulsions to be ternary mixtures of oil, water and surfactant. Space is divided into cubes of size ξ filled either with water or oil. The surfactant is constrained to stay at the water-oil interface; we divide it equally between the oil and water domains. Using the random mixing approximation, the probability ϕ for a cube to contain water is

$$\phi = \phi_w + \phi_s/2$$

where ϕ_w and ϕ_s are, respectively, the volume fractions of water and surfactant. The probability for a cube to contain oil is $1-\phi$. The constraint for the surfactant to fill the water-oil interface allows us to relate the volume fractions of the components and the lattice size ξ within the random mixing approximation:

$$\phi_s \Sigma_0 = z v_s \frac{\phi(1-\phi)}{\xi} \quad (2.1)$$

where $z=6$ is the coordination number of the cubic lattice; v_s is the molecular volume of the surfactant, and Σ_0 is the surface area per polar head of a surfactant molecule, which is fixed. Within this approximation the relation (2.1) gives the lattice size ξ at each point of the phase diagram

$$\frac{\xi}{a} = z \frac{\phi(1-\phi)}{\phi_s} \quad (2.2)$$

where $a = v_s / \Sigma_0$ is a molecular length. Note that in our model, the lattice size ξ is neither fixed at a constant value (as in the JLG model) nor a variational parameter (as in Widom's model) but is determined by the constraint, Eq. (2.2).

Since the area per polar head is fixed, the free energy per unit volume, f , has only two terms: the entropy of mixing of the water and oil domains, f_s , and the energy of curvature of the interface, f_c . The first term is calculated using the random mixing approximation¹⁷

$$f_s = \frac{T}{\xi^3} [\phi \log(\phi) + (1-\phi) \log(1-\phi)] = \frac{T}{\xi^3} S(\phi) \quad (2.3)$$

The second term f_c is calculated as follows. First we associate the bending energy E_c of a cube of water (oil) of size ξ surrounded by oil (water) with that of a sphere of diameter ξ

$$E_c = 8 \pi K(\xi) (1 - \xi / \rho_0)^2$$

where ρ_0 is twice the spontaneous radius of curvature (c_0^{-1} of Eq. (1.1)) and is defined to be positive for curvature towards the water and negative for curvature towards the oil. In our model the probability of having a bend is related to the probability of having an edge. However, we take the radius of curvature to be comparable to ξ , rather than presuming the interface to have a sharp edge. Thus, the total energy of curvature per unit volume is given by

$$f_c = \frac{8\pi K(\xi)}{\xi^3} [\phi(1-\phi)^2 (1 - \xi/\rho_0)^2 + \phi^2(1-\phi) (1 + \xi/\rho_0)^2] \quad (2.4a)$$

$$\approx \frac{8\pi K(\xi)}{\xi^3} \phi(1-\phi) [1 - 2\xi(1-2\phi)/\rho_0] \quad (2.4b)$$

In equation (2.4b), we have dropped a term linear in ϕ_s which may be absorbed into the chemical potential of surfactant.

As explained in Sec. I, we have explicitly incorporated in our model

the renormalization of the bending constant by thermal fluctuations. The bending constant $K(\xi)$ is then explicitly a function of the lattice size ξ , Eq.(1.4), and is a decreasing function of the lattice size ξ . The total free energy per unit volume, f , is the sum of f_s , Eq. (2.3), and f_c , Eq. (2.4b). We can rewrite the free energy in reduced units, defining

$$r = \alpha T / (4\pi K_0) \quad (2.5a)$$

$$\xi_K = a \exp(1/r) = a \delta \quad (2.5b)$$

$$x = \xi / \xi_K \quad (2.5c)$$

$$x_0 = \xi_K / \rho_0 \quad (2.5d)$$

$$\bar{\phi}_s = \phi_s \delta \quad (2.5e)$$

We also define the reduced free energy $f_r = (\xi_K^3 / T) f$

$$f_r = \frac{1}{x^3} \left\{ S(\phi) - 2\phi(1-\phi) \log(x) [1 - 2xx_0(1-2\phi)] \right\} \quad (2.6)$$

The constraint given by the Eq. (2.2) becomes

$$x = 6 \frac{\phi(1-\phi)}{\bar{\phi}_s} \quad (2.7)$$

Equations (2.6) and (2.7) define a reduced free energy $f_r(\phi, s)$ as a function of the two compositions ϕ and $\bar{\phi}_s$. This free energy is universal in the sense that, in reduced units, it does not depend on the value of K_0 . There is only one parameter: x_0 , the reduced curvature. All the lengths are in units of ξ_K and the energies in units of T .

B. Calculation of the Phase Diagram

To calculate the phase diagram, we define the potential:

$$g(\phi, \bar{\phi}_s) = f_r(\phi, \bar{\phi}_s) - \mu_\phi \phi - \mu_s \bar{\phi}_s \quad (2.8)$$

The equivalent of the common tangent construction on $f_r(\phi, \bar{\phi}_s)$ is the minimization of $g(\phi, \bar{\phi}_s)$ with respect to ϕ and $\bar{\phi}_s$ for fixed values of the chemical potentials μ_ϕ and μ_s . We solve the system of two equations defined by

$$\left(\frac{\partial g}{\partial \phi} \right)_{\phi_s} = 0 \quad \text{and} \quad \left(\frac{\partial g}{\partial \bar{\phi}_s} \right)_{\phi} = 0 \quad (2.9)$$

The absolute minimum of the function g corresponds to the stable phase at a given chemical potential. The technical details are explained in Ref. 33. The calculation for $x_0=0$ (no spontaneous curvature) leads to the phase diagram shown in Figure 1a. It exhibits a one phase region (the microemulsion phase) and three polyphasic regions: two two-phase regions where a microemulsion phase is in equilibrium with a very dilute phase of surfactant in water or oil, and a three-phase region where a middle-phase microemulsion is in equilibrium with both dilute phases.

Figure 1b is a plot of the value of $x=\xi/\xi_K$ along the two phase coexistence curve. The structural length ξ in the middle phase (for $\phi=0.5$) is proportional to ξ_K ($\xi \approx 0.23\xi_K$ for $\tau=0.2$). Moreover, ξ remains on the order of ξ_K even far from the middle phase. It is only when ϕ is very close to 0 or 1 that ξ falls rapidly to a microscopic value ($\xi \sim a$). In addition, the concentration of surfactant in the middle phase³⁴ scales as $\exp(-1/\tau)$. Thus the volume fraction of surfactant can be very small, when ξ_K is large compared to the molecular length. Consequently, the phase diagram is a strong function of ξ_K (and therefore of K_0).

The detailed structure in the corners of the phase diagram is given in the inset of Figure 1a. All the tie-lines of the two phase equilibria start from the boundaries of the phase diagram (water-surfactant and oil-surfactant sides). The points where the coexistence curves reach the limits of the phase diagram are critical points. Indeed at these points the composition of the two phases in equilibrium becomes identical³⁵. It should be noted, however, that we do not expect our free-energy to be accurate in this region of the phase diagram. We will see in the next section that we can generalize our model to include a more realistic account of the properties of the dilute phases.

We now consider the case of finite spontaneous curvature ($x_0 \neq 0$). We choose $x_0 > 0$; the case $x_0 < 0$ corresponds to the same evolution of the phase diagram but with the oil and water volume fractions interchanged. So long as the spontaneous radius of curvature remains larger or on the order of ξ_K ($x_0 < 1$) the phase diagram shows a slight asymmetry but the three-phase equilibrium still exists³³. However, when the spontaneous curvature x_0 is much greater than 1 ($\rho_0 \ll \xi_K$), the three-phase region vanishes (Figure 2). The phase diagram is then very asymmetric and the two-phase region consists

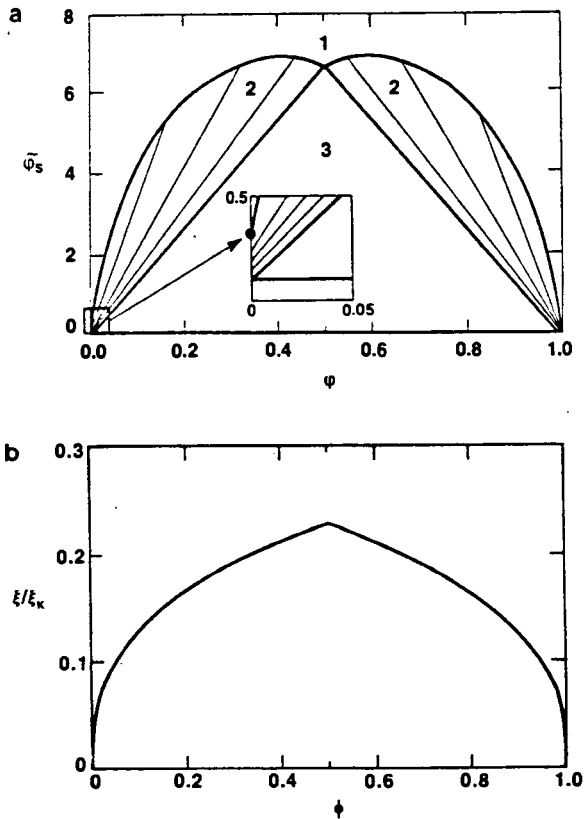


Figure 1. (a) Phase diagram for the case of no spontaneous curvature ($x_0 = 0$). The numbers denote the number of coexisting phases and the tie-lines in the two-phase regions are shown. The inset shows the details of the tie-lines at small values of the volume fractions. The values $r=0.2$ and $\alpha=1$ were chosen. (b) Variation of $x = \xi/\xi_k$ (the normalized length scale of the microemulsion) along the two-phase boundary of Fig. 1a.

of equilibria between a microemulsion phase and a phase that almost all water. In this case ξ is no longer proportional to ξ_K , but scales with ρ_0 , indicating that phase separation occurs when the typical domain size of the cube is of the order of ρ_0 . This result is an indication of the emulsification failure³ instability that precludes the formation of globules with a size larger than ρ_0 . It is also interesting to notice that the three-phase equilibrium disappears when $x_0 = \xi_K/\rho_0$ is of order unity.

III. EXTENSIONS OF THE BASIC MODEL

A. Generalized Phase Diagrams

The previous section described the phase diagram obtained from a double-tangent plane construction using the free energy of Eq.(2.6). We now describe a simplified method for generating the two- and three-phase coexistence regions. This method relies on the observation that the microemulsion phases coexist with very dilute phases of surfactant in water or in oil.

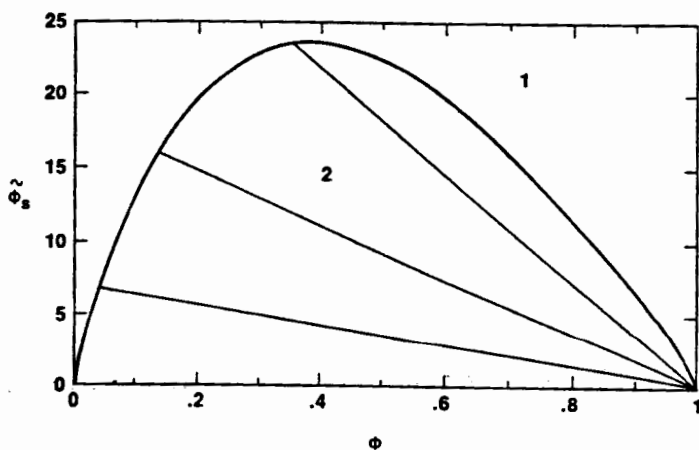


Figure 2. Phase diagram for finite spontaneous curvature, with $x_0 = 10$ and $r = 0.15$. The tie-lines in the two-phase region indicate coexistence of a phase which is mostly water with a microemulsion phase. The three-phase region no longer exists for this value of x_0 .

Our study of the free energy surface³³ showed that the three-phase equilibrium is due to the presence of two deep minima in the model free energy, in the region of very small surfactant concentration. However our model, which describes the surfactant as an almost flat monolayer at the water/oil interface, is not really appropriate in the dilute regime where these minima occur. It is unreasonable to extrapolate the bending energy to dilute phases where the surfactant exists in the form of micelles or isolated molecules in solution.

We, therefore, introduce a simple model for these dilute phases which is, in general, not merely an extrapolation of the microemulsion free energy. Denoting the free energy per unit volume of the dilute phases in water and oil respectively by \bar{F}_w and \bar{F}_o , we write

$$\bar{F}_w = T \left[\bar{\phi}_s (\log \bar{\phi}_s - 1) + \kappa_w \bar{\phi}_s \right] / R^3 \quad (3.1)$$

where $\bar{\phi}_s$ is the volume fraction of surfactant in the dilute phase and R^3 is the volume of a micelle. The first term in Eq.(3.1) is the entropy of mixing and the second term is the energy of surfactant in dilute solution. Note that the zero of energy is that of a flat surfactant monolayer. Thus, if the surfactant free energy is lowest for saturated interfaces, the dimensionless energy κ_w of the micelle or isolated surfactant in solution is positive³⁶. It is only the entropy of mixing that stabilizes these dilute phases with respect to the monolayer-like microemulsion phases. A similar expression is used for the free energy per unit volume of the oil-rich dilute phases with $\bar{F}_w \rightarrow \bar{F}_o$ and $\kappa_w \rightarrow \kappa_o$.

Since we expect³⁷ $R \sim a$, we see that the dilute limit of our microemulsion free energy, Eq.(2.6) with $x_o=0$, reduces to the form of Eq.(3.1), when $\kappa_w \gg 1$, with $R=6^{1/3} a$, and with $\kappa_w=8\pi K_o/T$. The recognition that the dilute phases cannot necessarily be described by the same harmonic bending energy as the microemulsion phases is expressed by the introduction of a new energy κ_w , which is not simply related to K_o .

Recalling the coexistence curves of Figure 1, we now look for an equilibrium of a three-component microemulsion with a two-component, dilute phase. The equations for two-phase equilibrium of the microemulsion with a dilute phase of surfactant in water are:

$$f + (1-\phi) \frac{\partial f}{\partial \phi} - \phi_s \frac{\partial f}{\partial \phi_s} = \bar{f}_w - \bar{\phi}_s \frac{d\bar{f}_w}{d\bar{\phi}_s} \quad (3.2)$$

$$\frac{\partial f}{\partial \phi_s} - \frac{1}{2} \frac{\partial f}{\partial \phi} = \frac{d\bar{f}_w}{d\bar{\phi}_s} \quad (3.3)$$

Equation (3.3) results from the equality of the chemical potential for surfactant which exists in both the microemulsion and dilute phases. The second term in Eq.(3.3) arises from the dependence of ϕ in the microemulsion phase on ϕ_s . For a dilute phase of surfactant in water, Eqs.(3.1) and (3.3) determine the value $\bar{\phi}_s = \phi_s^*$ at coexistence as

$$\log \phi_s^* = -\kappa_w + \left[\frac{\partial f}{\partial \phi_s} - \frac{1}{2} \frac{\partial f}{\partial \phi} \right] / T \quad (3.4)$$

Since f in the microemulsion phase is of order T/ξ_K^3 , where $\xi_K/a - \exp(1/\tau) \gg 1$, and since $\phi_s \sim 1/\xi_K$ in the middle phase, the second term on the right hand side of Eq. (3.4) is of the order of $1/\xi_K^2$. Thus, for large values of ξ_K , the first term on the right hand side of Eq.(3.4) dominates. Equation (3.4) shows that the value of ϕ_s^* in the dilute phases is approximately independent of the value of ϕ or ϕ_s in the coexisting microemulsion phases.

Similar considerations allow us to neglect the second term on the right hand side of Eq. (3.2). With these approximations, the above equations reduce to only one condition:

$$f + (1-\phi) \frac{\partial f}{\partial \phi} - \phi_s \frac{\partial f}{\partial \phi_s} = f_w^* \quad (3.5)$$

where now $f_w^* = \bar{f}_w(\phi_s^*)$, with $\phi_s^* = \exp(-\kappa_w)$. The phase boundary for two-phase coexistence is then found directly by plotting ϕ_s as a function of ϕ as given by Eq.(3.5). If the value $\kappa_w = 8\pi K_0/T$ is used, the results are indistinguishable from those of the tangent plane construction (see Figure 1), except for a region very close to the corners of the phase diagram. Our approximation is equivalent to having the ends of the tie-lines in Figure 1 meet at a single point. By choosing different values of κ_w and κ_0 , we can generalize the previous results. Note that Eq.(3.1) can be generalized to

even more accurately model the free energy of the dilute-phases. For example, the inclusion of attractive interactions will further destabilize the micellar phase.

We have just described a simplified generalization for determining the coexistence of a microemulsion with dilute phases of surfactant in water or oil. The independent modeling of the free energy of dilute surfactant solutions introduces two more relevant energy scales, κ_w and κ_o in addition to K_o . Since $f_w^* \sim T \exp(-\kappa_w) / a^3$, we can equally well parameterize the dilute phases by their values of f_w^* or f_o^* . The coexistence curves are in general sensitive to the values of these parameters. For example, Figure 3 shows that if $f_w^* \neq f_o^*$, the phase diagram is not symmetric about $\phi=0.5$, even though the microemulsion phase has no preferred curvature ($x_o=0$). This is because phase equilibria are sensitive to the global properties of the free energy surface. Although there is no spontaneous bending of a surfactant film towards either water or oil, the different free energies of isolated surfactant molecules or micelles in water-rich and oil-rich environments can be different. If f_w^*/f_o^* is very different from unity, the three-phase region can entirely disappear. There are thus two mechanisms which can give rise to an asymmetry of the phase diagram, and in the extreme case, to the disappearance of the three-phase equilibrium: (i) a finite spontaneous curvature, (ii) a difference in the free energies of the surfactant in the dilute phases (f_w^*, f_o^*).

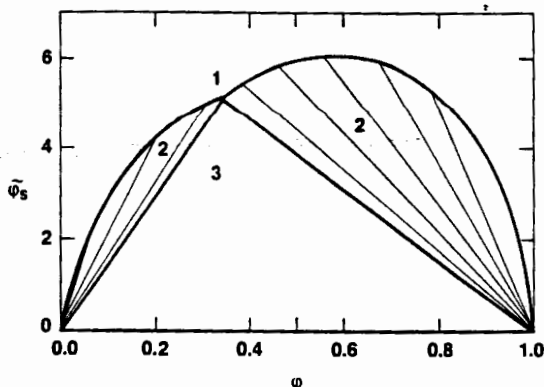


Figure 3. Phase diagram for no spontaneous curvature ($x_o = 0$), but with asymmetry in the free energies of the dilute phases ($f_w^* \neq f_o^*$). Here, $f_w^* = -15T/\xi_K^3$ and $f_o^* = -15 T/2\xi_K^3$.

B. The Lamellar Phase

In this section, we consider the relative stability of random microemulsions compared with a lamellar phase which consists of an ordered array of surfactant monolayers dividing adjacent oil and water domains. For the case of no spontaneous curvature, we show that for values of K_0/T that are not too large, the random microemulsion is more stable than the lamellar phase at small values of ϕ_s . The renormalization of the bending constant to values of the order of T , allows the energy cost of the random system to be compensated by the entropy gain from the random mixing of water and oil regions. At large values of ϕ_s , the bending constant approaches its bare value, K_0 . The energy cost of the curved interfaces in the random microemulsion is no longer compensated by the entropy of mixing, and the lamellar phase dominates.

We compare the free energies of the microemulsion and lamellar phases³⁸. Although the ordered, lamellar phase has no entropy of mixing and approximately no curvature energy, it has a finite free energy due to the steric repulsion of the surfactant sheets^{39,40}. This repulsion reduces the meandering entropy of the lamellae from its value in the limit of infinite separation of the surfactant sheets. The additional free energy per unit volume has been estimated by Helfrich³⁹ for a two-component system, and can be approximately generalized to describe the free energy per unit volume of the lamellar microemulsion, f_l .

$$f_l = \chi T \left[\frac{T}{K_0} \right] \left[\frac{2}{d_o + d_w} \right] \left[\frac{1}{d_o^2} + \frac{1}{d_w^2} \right] \quad (3.6)$$

In Eq. (3.6), $d_o \approx 2a\phi_o/\phi_s$ and $d_w \approx 2a\phi_w/\phi_s$ are the distances between the surfactant sheets separating oil and water domains, respectively. The surfactant volume fraction is given by $\phi_s = 2a/(d_o + d_w) = a/d$. We expect Eq. (3.6) to be correct for $d < \xi_K$. The parameter χ in Eq. (3.6) expresses the uncertainty in the numerical coefficient of Eq. (3.6) which depends on the details of the short distance cutoff. In our numerical calculations, we take $\chi = 0.15/\pi \approx 0.05$; if χ is taken to be Helfrich's value of $\chi = 0.3$, the microemulsion is more stable than the lamellar phase even at high values of ϕ_s .

The phase diagram is obtained from a double tangent construction on both f_l and f as described in Sec. II above. The results are shown in Figure 4, for a value of $\tau = T/4\pi K_0 = 0.2$. Since the lamellar free energy

scales as $(T^2/K_0) \phi_s^3/a^3$ and the microemulsion free energy scales as $T \phi_s^3/a^3$, the free energy difference between them decreases as K_0 is increases. For large values of K_0/T , the lamellar phase is more stable than the random microemulsion phase and the middle-phase along with the three-phase equilibrium disappears. This confirms the suggestion of de Gennes-Taupin¹⁶, that the lamellar structure is more stable than the random microemulsion for stiff surfactant sheets.

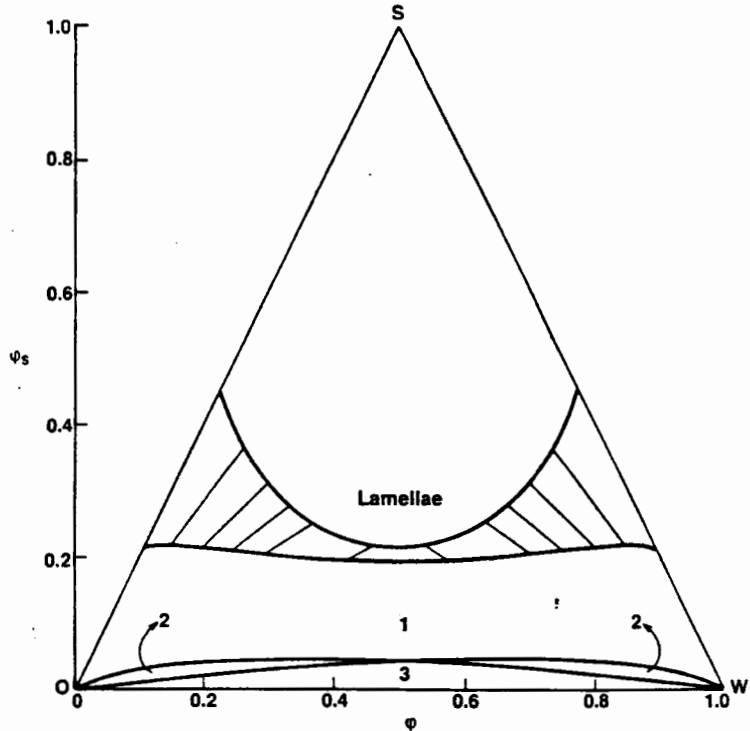


Fig. 4. Phase diagram for microemulsions with no spontaneous curvature. The region where the lamellar phase is stable is indicated; the numbers indicate the number of coexisting phases. A value of $\tau=0.2$ was chosen. The tie-lines indicate the coexistence of disordered microemulsion phases with lamellar phases. The lower part of this phase diagram is the same as in Fig. 1a, but with a different vertical scale since $\tilde{\phi}_s = \phi_s \exp(1/\tau)$. The phase diagram is drawn within the triangle of allowed concentrations: $\phi_s < \phi/2$, $\phi_s < (1-\phi)/2$, and the corners S, W, and O correspond to pure surfactant, water, and oil respectively.

This comparison of the free energies of the lamellar and microemulsion phases reveals the crucial nature of the renormalization of the bending constant. It is through this renormalization that the bending energy in the random microemulsion phase is reduced so that the entropy gain of the random structure stabilizes it against the ordered lamellar phase.

IV. DISCUSSION

We now make a few remarks about our resulting phase diagrams and compare them with previous models:

(i) In the symmetric case ($x_0 = 0$) the calculated phase diagram, Fig. 1, has four distinct regions: a single phase, two two-phase coexistence regions (one consisting of a microemulsion in equilibrium with a phase which is almost all water and the other of a microemulsion in equilibrium with a phase which is almost all oil) and a three-phase coexistence region where the middle phase microemulsion is in equilibrium with both water and oil. The surfactant concentration in the middle phase is inversely proportional to the persistence length and hence depends exponentially on the bending constant K_0 .

(ii) Deviations from this symmetric picture are observed as we change the spontaneous curvature x_0 from zero to a finite positive (negative) value which reflects a tendency of the surfactant to bend towards the water (the oil). As one increases x_0 from zero, the middle phase moves towards the oil corner. Consequently, the extent of the two-phase coexistence with the water increases while the extent of the two-phase coexistence with the oil decreases until it, as well as the three phase region, completely disappears, Figure 2, leaving only the two-phase coexistence between the microemulsion (globules of water in oil) and an excess water phase. This happens at values of $\rho_0 \leq f_K$ and is in agreement with the concept of an "emulsification failure" instability that was previously discussed for globular microemulsions⁵.

With the simple expression that we have for the free energy, Eq. (2.6), ρ_0 (or x_0) is the only parameter that affects the asymmetry of the phase diagram. In Sec. III, we generalized our model and introduced two additional parameters, f_w^* and f_o^* , which are the values of the free energy minima in the dilute water and oil phases, and are related to the surfactant stability in those phases. In the generalized model, another way to asymmetrize the phase diagram, Figure 3, is to increase $|f_w^* - f_o^*|$ while keeping both minima below

the microemulsion value. For example, increasing the value of f_w^* with respect to f_o^* causes a shrinkage of the two-phase coexistence with oil until this coexistence region, as well as that of the three-phase coexistence, disappear.

(iii) Our theory contains several phenomenological parameters such as x_o , f_w^* , and f_o^* which are related to the surfactant structure and chemistry. These parameters can asymmetrize the phase diagram; they are experimentally controlled through changes in the hydrophilic-lipophilic ratio⁴¹ which can be brought about by changes in temperature (which has other effects as well), salinity, and the stability of the dilute phase of surfactant in water and oil⁴². Since salinity screens the electrostatic interaction in the water, it can be thought of as decreasing x_o in our model. Also our simplified account of the stability of the water and oil in terms of the two parameters f_w^* and f_o^* , shows that as the stability of the oil increases, the oil-microemulsion coexistence region shrinks, until only an equilibrium with water is left (no three-phase region). The reverse behavior is seen when the water stability is increased.

(iv) Another change in the phase diagram occurs as one increases the value of $f_w^* - f_o^* = f^*$ with respect to the microemulsion free energy. For f^* near zero, the system prefers³³ to separate into two microemulsions, one being oil-rich and the other water-rich (with equal amount of surfactant for the symmetric case $x_o = 0$). Consequently, the entire three-phase region disappears. This again shows the importance of f^* to the existence of the three-phase region. A similar two-phase coexistence between two microemulsions was also obtained by de Gennes and Taupin and by JLG. In their model, it was not possible to obtain the three-phase region because the cell size was always presumed to be equal to ξ_K , the persistence length; whereas in our model, the cell size varies from $\xi - \xi_K$, near the middle-phase point on the phase diagram, to a molecular size for the dilute phases. As in the JLG model, we find³³ coexistence between two microemulsions with unequal amounts of surfactant (oblique tie-lines) by introducing a finite spontaneous curvature.

(v) Although both our model²⁹ and Widom's¹⁸ result in three-phase coexistence, there are several important differences between them. In Widom's model the surfactant film is thought of as highly compressible two-dimensional gas whereas in our model it is an incompressible film. The stability of the undulating interface in our case is a direct consequence of the renormalization of the bending constant and we find that the structural

length scale (cell size) ξ is closely related to the de Gennes-Taupin persistence length ξ_K . In the middle phase, ξ is proportional to ξ_K ; along the two-phase coexistence lines, Figure 1b, it deviates strongly from ξ_K only very close to the corners of the phase diagram. This exponential dependence of the cell size on the bending constant is not found by Widom. Rather in his case (for rigid surfactant films, $K_0 \gg T$) ξ depends¹⁸ only weakly on the bending constant, and exponentially on the water/oil bare surface tension. This difference between the two theories can be checked experimentally since (within the random mixing approximation) ξ is inversely proportional to ϕ_s the volume fraction of the surfactant. Measurements of K_0 versus ϕ_s will be helpful in comparing these two predictions.

(vi) The microemulsion phase should always be compared in stability to more ordered structure such as lamellae. This was done in Sec. III with some simplifying assumptions about the contribution of thermal fluctuations to the free energy of the lamellar phase. We find that for K_0/T larger than a critical value, the lamellar phase is always more stable than the microemulsion phase and the three-phase coexistence disappears altogether. In contrast, for K_0/T smaller than the critical value, the microemulsion phase is more stable than the lamellar phase for small ϕ_s ; as ϕ_s increases, there is a transition (always first order in our model because we are comparing two different branches of the free energy) from an isotropic disordered (microemulsion) phase at small values of ϕ_s to a lamellar one at higher values of ϕ_s . In the coexistence region, the two phases have different values of ϕ and ϕ_s , resulting in the oblique tie-lines in Figure 4.

V. CONCLUSIONS AND FUTURE PROSPECTS

In this paper, we focused on understanding the origin of middle phase microemulsions. Within a simple model we calculated phase diagrams that are similar to those observed for nonionic surfactant microemulsions⁴¹. In addition, our model has a simple physical explanation in terms of the statistics of the undulating surfactant films separating oil and water regions. The renormalization of the bending constant of such a film appears to be crucial to the stabilization of these phases. In the absence of renormalization of the bending constant, the phase diagram still shows a three-phase equilibrium, similar to that of Ref. 18. However, in that model, the length scale of the microemulsion in the middle phase is unrelated to the properties of the surfactant film (e.g., the persistence length). In addition, the free energy is greater than that of a lamellar phase.

Several points deserve additional study:

(i) Our calculation as well as those of Refs. 6,17, and 18 are done within the random mixing approximation, which does not take correctly into account concentration fluctuations. For small length scales (smaller than a cell size), fluctuations were included via the renormalization of the bending constant. However, one would like to find corrections to the mean field approximation for large length scales by writing down a lattice model where the entropy and the bending energy are better approximated.

(ii) In addition, the expression used for $K(\xi)$ was derived^{30,31} to first order in perturbation theory for zero surface tension interfaces. This expression is not expected to hold for large length scales. Even within first-order perturbation theory, there is a dispute^{30,31,32} at the present time about the exact value of coefficient α in the expression for $K(\xi)$. Changing α has a similar effect on our phase diagram as changing f^* (see Sec. III). Variations in either parameter can cause a crossover from three-phase equilibrium to coexistence between two different microemulsions. Our model has shown that the fluctuations of a random surface have a profound effect on the phase stability of random microemulsions. A more detailed theory of the random surface will enable a more complete application of these ideas.

ACKNOWLEDGMENTS

The authors acknowledge useful discussions with P.G. de Gennes, R. Goldstein, J. Huang, M.W. Kim, D. Langevin, S. Leibler, R. Reed, C. Safinya, and B. Widom.

REFERENCES

- (a) Permanent address: Centre Paul Pascal, C.N.R.S., Domaine Universitaire, 33405 Talence Cedex, France
- (b) Also at: Laboratoire de Physique de la matière condensée, Collège de France, 75231 Paris Cedex 05, France; Permanent address: School of Physics and Astronomy, Tel Aviv University, Ramat-Aviv, 69978 Israel.
- (c) Permanent address: Cavendish Laboratory, Madingley Road, Cambridge CB3 0HW, United Kingdom.

1. For a general survey, see (a) K. L. Mittal and B. Lindman, editors, "Surfactants in Solution", Vols. 1-3, (Plenum Press, New York, 1984); (b) K. L. Mittal and P. Bothorel, editors, "Surfactants in Solution", Vols. 4-6, (Plenum Press, New York, 1986); (c) S. A. Safran and N. A. Clark, editors, "Physics of Complex and Supermolecular Fluids", (Wiley, New York, 1987).
2. A. Calje, W.G.M. Agterof, A. Vrij in "Micellization, Solubilization, and Microemulsions", K. Mittal, editor, Vol. 2, p. 779 (Plenum Press, New York, 1977); R. Ober and C. Taupin, J. Phys. Chem. 84, 2418 (1980); A.M. Cazabat and D. Langevin, J. Chem. Phys. 74, 3148 (1981); D. Roux, A.M. Bellocq, P. Bothorel in Ref. 1a, p. 1843; J.S. Huang, S.A. Safran, M.W. Kim, G.S. Grest, M. Kotlarchyk, N. Quirke, Phys. Rev. Lett. 53, 592 (1983); M. Kotlarchyk, S. H. Chen, J.S. Huang, M.W. Kim, Phys. Rev. A 29, 2054 (1984).
3. (a) S.A. Safran and L.A. Turkevich, Phys. Rev. Lett. 50, 1930 (1983); (b) S.A. Safran, L.A. Turkevich, and P.A. Pincus, J. Phys. (Paris) Lett. 45, L69 (1984).
4. S.A. Safran, J. Chem. Phys. 78, 2073 (1981) and in Ref. 1a, p. 1781.
5. C. Huh, J. Colloid Interface Sci. 97, 201 (1984) and 71 (1979).
6. Y. Talmon and S. Prager, J. Chem. Phys. 69, 2984 (1978), and *ibid* 76, 1535 (1982).
7. L.E. Scriven, in "Micellization, Solubilization, and Microemulsions", K. Mittal, editor, Vol.2, p. 877 (Plenum Press, New York, 1977).
8. L. Auvray, J.P. Cotton, R. Ober, C. Taupin, J. Phys. (Paris) 45, 913 (1984) and in Ref. 1c.
9. E.W. Kaler, K.E. Bennett, H.T. Davis, L.E. Scriven, J. Chem. Phys. 79, 5673 and 5685 (1983); N.J. Chang and E.W. Kaler, Langmuir 2, 184 (1986).
10. A.M. Cazabat, D. Langevin, J. Meunier, A. Pouchelon, Adv. Colloid Interface Sci. 16, 175 (1982).
11. P. Ekwall, in "Advances in Liquid Crystals", G.H. Brown, editor, Vol. I, p. 1 (Academic Press, New York, 1975); A. M. Bellocq and D. Roux, in "Microemulsions", S. Friberg and P. Bothorel, editors (CRC Press, Boca Raton, FL, 1986); D.H. Smith, J. Colloid Interface Sci. 102, 435 (1984).
12. The terminology upper, lower, and middle arises from the position occupied by the microemulsion in the test tube.
13. L.A. Turkevich, S.A. Safran, and P. A. Pincus, in Ref. 1b, Vol 6, p. 1177.
14. H. Saito and K. Shinoda, J. Colloid Interface Sci., 32, 647 (1970); D. Guest and D. Langevin, J. Colloid Interface Sci. 112, 208 (1986); E. Ruckenstein and J. Chi, J. Chem. Soc. Faraday Trans. 2, 71, 1690 (1975).

15. See Proceedings of SPE/DOE Fifth Symposium on Enhanced Oil Recovery, Vols. 1-2, Tulsa, OK, April, 1986, Society of Petroleum Engineers.
16. P. G. de Gennes and C. Taupin, J. Phys. Chem. 86, 2294 (1982).
17. J. Jouffroy, P. Levinson, P.G. de Gennes, J. Phys. (Paris) 43, 1241 (1982).
18. B. Widom, J. Chem. Phys. 81, 1030 (1984).
19. G. L. Gaines, editor, "Insoluble Monolayers at Liquid-Gas Interfaces", (Wiley, New York, 1966).
20. J.C. Wheeler and B. Widom, J. Am. Chem. Soc. 90, 3064 (1968).
21. B. Widom, J. Chem. Phys. 84, 6943 (1986).
22. M. Schick and W.H. Shih, Phys. Rev. B 34, 1797 (1986); K. Chen, C. Ebner, C. Jayaprakash, and R. Pandit, J. Phys. C 20, L361 (1987).
23. Despite this large correlation length, the system is not in general near any kind of critical point. Under these conditions, it is a difficult mathematical task to extract the relevant behavior from a microscopic Hamiltonian.
24. Also, it may be difficult to eliminate spurious effects arising from the underlying lattice. For example, it is difficult to count bending energies correctly with a local Hamiltonian, operating on discrete spin-like variables. The bending energy of a surfactant-covered spherical globule of oil is independent of its size, R . On a cubic lattice, however, the corresponding state of lowest bending energy is a cube, which has a bending energy proportional to R/a , with a being the lattice spacing. One way to eliminate this kind of discrepancy is to choose the lattice spacing to be of the same order as the domain size R . This is, however, tantamount to taking the phenomenological approach.
25. Experiments have shown that the area per head is approximately constant along the coexistence curves - see Ref. 8.
26. W. Helfrich, Z. Naturforsch. 28a, 693 (1973).
27. S.J. Candau, E. Hirsch, and R. Zana, J. Colloid Interface Sci. 105, 521 (1984).
28. T. Imae and S. Ikeda, J. Coll. Interface Sci. 99, 300 (1984).
29. S.A. Safran, D. Roux, M. Cates, and D. Andelman, Phys. Rev. Lett. 57, 491 (1986).
30. W. Helfrich, J. Phys. (Paris) 46, 1263 (1985) and 48, 285 (1987).
31. L. Peliti and S. Leibler, Phys. Rev. Lett. 54, 1690 (1985).
32. D. Forster, Phys. Lett. 114A, 115 (1986); W. Kleinert, Phys. Lett. 114A, 263 (1986)

33. D. Andelman, M. Cates, D. Roux, and S.A. Safran, J. Chem. Phys. 87, 7229 (1987); also in Langmuir (in press).
34. This is also the minimum amount of surfactant needed to obtain a one-phase microemulsion with the same amount of water and oil in the context of our free energy.
35. This critical point is in fact a tricritical point whose nature is the same as the tricritical points of Widom's model(see Ref. 18).
36. Since $\kappa_w > 0$, a concentrated micellar phase where the entropy is negligible is itself unstable and would probably coexist with a lamellar phase.
37. This is true for micellar phases where the globules are compact.
38. This is appropriate because our microemulsion free energy, f , considered only the change in f due to bending.
39. W. Helfrich, Z. Naturforsch. 33a, 305 (1978).
40. C.R. Safinya, D. Roux, G.S. Smith, S.K. Sinha, P. Dimon, N.A. Clark, and A.M. Bellocq, Phys. Rev. Lett. 37, 2718 (1986).
41. D.H. Smith, J. Colloid Interface Sci. 102, 435 (1984), 108, 471 (1985); M. Kahlweit, R. Strey, and P. Firman, J. Phys. Chem. 90, 671 (1986).
42. Other changes involve discrete changes in the type of surfactant, hydrophile and lipophile size, number of carbon double bonds, aromaticity of the oil, etc..